

The NUMEN Project: Toward new experiments with high-intensity beams

*Original*

The NUMEN Project: Toward new experiments with high-intensity beams / Agodi, C.; Russo, A. D.; Calabretta, L.; D'Agostino, G.; Cappuzzello, F.; Cavallaro, M.; Carbone, D.; Finocchiaro, P.; Pandola, L.; Torresi, D.; Calvo, D.; Sartirana, D.; Campajola, L.; Capirossi, V.; Iazzi, F.; Pinna, F.. - In: UNIVERSE. - ISSN 2218-1997. - ELETTRONICO. - 7:3(2021), p. 72. [10.3390/universe7030072]

*Availability:*

This version is available at: 11583/2931624 since: 2021-10-15T10:04:46Z

*Publisher:*

MDPI AG

*Published*

DOI:10.3390/universe7030072

*Terms of use:*








This article is made available under terms and conditions as specified in the corresponding bibliographic description in the repository

*Publisher copyright*

(Article begins on next page)

## Article

# The NUMEN Project: Toward New Experiments with High-Intensity Beams

Clementina Agodi <sup>1,\*</sup>, Antonio D. Russo <sup>1</sup>, Luciano Calabretta <sup>1</sup>, Grazia D'Agostino <sup>1</sup>, Francesco Cappuzzello <sup>1,2</sup>, Manuela Cavallaro <sup>1</sup>, Diana Carbone <sup>1</sup>, Paolo Finocchiaro <sup>1</sup>, Luciano Pandola <sup>1</sup>, Domenico Torresi <sup>1</sup>, Daniela Calvo <sup>3</sup>, Diego Sartirana <sup>3</sup>, Luigi Campajola <sup>4</sup>, Vittoria Capirossi <sup>3,5</sup>, Felice Iazzi <sup>3,5</sup> and Federico Pinna <sup>3,5</sup> for the NUMEN Collaboration

- <sup>1</sup> Laboratori Nazionali del Sud, Istituto Nazionale di Fisica Nucleare, 95123 Catania, Italy; antonio.russo@lns.infn.it (A.D.R.); calabretta@lns.infn.it (L.C.); dagostino@lns.infn.it (G.D.); cappuzzello@lns.infn.it (F.C.); manuela.cavallaro@lns.infn.it (M.C.); carboned@lns.infn.it (D.C.); finocchiaro@lns.infn.it (P.F.); pandola@lns.infn.it (L.P.); torresi@lns.infn.it (D.T.)
- <sup>2</sup> Dipartimento di Fisica e Astronomia 'Ettore Majorana', Università di Catania, 95123 Catania, Italy
- <sup>3</sup> INFN, Sezione di Torino, 10124 Torino, Italy; calvo@to.infn.it (D.C.); diego.sartirana@to.infn.it (D.S.); vittoria.capirossi@polito.it (V.C.); felice.iazz@polito.it (F.I.); fpinna@to.infn.it (F.P.)
- <sup>4</sup> Dipartimento di Fisica—Università di Napoli Federico II, Napoli 80138 Italy, INFN Sezione Napoli, 80126 Napoli, Italy; luigi.campajola@unina.it
- <sup>5</sup> DISAT, Politecnico di Torino, 10129 Torino, Italy
- \* Correspondence: agodi@lns.infn.it



**Citation:** Agodi, C.; Russo, A.D.; Calabretta, L.; D'Agostino, G.; Cappuzzello, F.; Cavallaro, M.; Carbone, D.; Finocchiaro, P.; Pandola, L.; Torresi, D.; et al. The NUMEN Project: Toward New Experiments with High-Intensity Beams. *Universe* **2021**, *7*, 72. <https://doi.org/10.3390/universe7030072>

Academic Editor: Jouni Suhonen

Received: 21 January 2021

Accepted: 16 March 2021

Published: 22 March 2021

**Publisher's Note:** MDPI stays neutral with regard to jurisdictional claims in published maps and institutional affiliations.



**Copyright:** © 2021 by the authors. Licensee MDPI, Basel, Switzerland. This article is an open access article distributed under the terms and conditions of the Creative Commons Attribution (CC BY) license (<https://creativecommons.org/licenses/by/4.0/>).

**Abstract:** The search for neutrinoless double-beta ( $0\nu\beta\beta$ ) decay is currently a key topic in physics, due to its possible wide implications for nuclear physics, particle physics, and cosmology. The NUMEN project aims to provide experimental information on the nuclear matrix elements (NMEs) that are involved in the expression of  $0\nu\beta\beta$  decay half-life by measuring the cross section of nuclear double-charge exchange (DCE) reactions. NUMEN has already demonstrated the feasibility of measuring these tiny cross sections for some nuclei of interest for the  $0\nu\beta\beta$  using the superconducting cyclotron (CS) and the MAGNEX spectrometer at the Laboratori Nazionali del Sud (LNS) Catania, Italy. However, since the DCE cross sections are very small and need to be measured with high sensitivity, the systematic exploration of all nuclei of interest requires major upgrade of the facility. R&D for technological tools has been completed. The realization of new radiation-tolerant detectors capable of sustaining high rates while preserving the requested resolution and sensitivity is underway, as well as the upgrade of the CS to deliver beams of higher intensity. Strategies to carry out DCE cross-section measurements with high-intensity beams were developed in order to achieve the challenging sensitivity requested to provide experimental constraints to  $0\nu\beta\beta$  NMEs.

**Keywords:** neutrinoless double beta decay; nuclear double-charge exchange reactions; superconducting cyclotron; magnetic spectrometer; high-intensity beams

## 1. Introduction

The strong interest in the double-beta decay processes began in 1939, when Wendell Furry [1], starting from the work of Maria Goeppert-Mayer [2], applied the neutrino model previously proposed by Ettore Majorana [3], in which there is no distinction between particle and antiparticle and which proposes a new hypothetical decay, now known as neutrinoless double-beta ( $0\nu\beta\beta$ ) decay.

The  $0\nu\beta\beta$  decay is a hypothetical class of nuclear processes where a parent nucleus is transformed into an isobar daughter differing by two-unit charges and two electrons (or positrons) are emitted. Although still not observed, these phenomena are nowadays being strongly investigated since, if discovered in the experiments, they would allow one to directly determine the Majorana nature of the neutrino and to confirm that the total lepton number is not always conserved in nature [3]. Moreover, the neutrino effective mass

would be extracted from decay rate measurements, with foreseen sensitivity to normal or inverted hierarchy scenarios in the neutrino mass distribution. Presently, this physics case is leading the research “beyond the standard model” and could open new perspectives toward a grand unified theory of fundamental interactions and contribute to explaining the matter–antimatter asymmetry observed in the universe.

The search for  $0\nu\beta\beta$  decay is a worldwide race. Many projects are competing in the challenge to detect such a hypothetical decay: the CUORE/CUPID project [4] and LEGEND/GERDA [5] at the INFN-LNGS, in Italy; EXO/nEXO [6] at WIPP, in the USA; KamLAND-Zen [7] and CANDLES at Kamioka, Japan [8]; the SNO at Sudbury, in Canada [9]; AMoRe in Korea [10]; SuperNEMO at the LSM, in France [11], etc.

The  $0\nu\beta\beta$  half-life critically depends on the nuclear matrix element (NME) that controls the decay,  $M_{0\nu\beta\beta}$  [12–14]. Since the decay involves nuclei, its determination necessarily implies structural issues in the nuclei embedded in the NMEs. A deeper knowledge of the NMEs is therefore crucial to infer the neutrino mass from experimental measurements (or constraints) of the  $0\nu\beta\beta$  decay rate and to develop the design strategies of future experiments.

Significant differences are found in NME calculations obtained with different nuclear structure models [13,15–17]. This fact makes the determination of NMEs based on different calculation schemes controversial, given also the lack of experimental constraints.

In this context, the NUMEN project [18–21] aims to obtain quantitative information on the NMEs of  $0\nu\beta\beta$  decay by measuring heavy ion–DCE reaction cross sections. The measurements of the DCE cross sections are performed using the K800 Superconducting Cyclotron to accelerate beams and the MAGNEX large acceptance magnetic spectrometer to detect the ejectiles, at the INFN-LNS laboratory in Catania, Italy [22]. The characteristic feature of these reactions is the transfer of two charge units that leaves the mass number unchanged. They can proceed both by a sequential nucleon-transfer mechanism and by the exchange of two isovector mesons, in an uncorrelated or correlated way [23,24]. Although the DCE and  $0\nu\beta\beta$  decay processes are mediated by different interactions, there are several important similarities [25], as follows:

- Parent/daughter states of the  $0\nu\beta\beta$  decay are the same as those of the target/residual nuclei in the DCE.
- Short-range Fermi, Gamow–Teller, and rank-2 tensor components are present in both transition operators, with relative weight depending on incident energy in the DCE. Performing the DCE experiments at different bombarding energies is essential to gaining sensitivity on the individual contribution of each component.
- A large linear momentum ( $\approx 100$  MeV/c) is available in the virtual intermediate channel of both processes. This is a distinctive similarity since other processes, such as single- $\beta$  decay,  $2\nu\beta\beta$  decay, and light-ion-induced single-charge exchange (SCE), cannot probe this feature. An interesting development is the recently proposed  $\mu$ -capture experiment at Research Center of Nuclear Physics (RCNP), Osaka Japan [26].
- The two processes are non-local and are characterized by two vertices localized in a pair of valence nucleons.
- Both processes take place in the same nuclear medium. In-medium effects are expected to be present in both cases, so DCE data could give a valuable constraint on the theoretical determination of quenching phenomena in  $0\nu\beta\beta$  decay.
- Off-shell propagation through virtual intermediate channels is present in both cases.

An important issue of the DCE, not present in  $0\nu\beta\beta$  decay, is the contribution coming from multi-nucleon transfer reactions, representing a competitive route with respect to direct exchange and leading to the same final states. The effects of multi-nucleon transfer start from the 4th order in the nucleon–nucleon potential since two protons (neutrons) should be stripped from the projectile and two neutrons (protons) picked up from the target. In ref. [21], it is shown that, under the experimental conditions expected for the campaign at the INFN-LNS, the contribution of multi-nucleon transfer is negligible (less than 1%). Similar results are being found in the preliminary analysis of the other pilot

cases. Consequently, the leading DCE reaction mechanism is connected to nucleon–nucleon isovector interaction, which acts between two neutrons in the projectile and two protons in the target for the ( $^{18}\text{O},^{18}\text{Ne}$ ) and between two protons in the projectiles and two neutrons in the target for the ( $^{20}\text{Ne},^{20}\text{O}$ ) reaction. A useful way to describe the DCE process is by means of the exchange of two charged  $\pi$  or  $\rho$  mesons between the involved nucleons. An interesting question is whether the two mesons are exchanged independently of each other, in analogy to  $2\nu\beta\beta$  decays, or in a correlated way, as in  $0\nu\beta\beta$  decays. This question is very relevant for the connection of DCE reactions to  $0\nu\beta\beta$  decays. This aspect is also important from the point of view of nuclear reaction theory, since it could indicate a new way to access nucleon–nucleon short-range correlations [23].

Aiming for a systematic study of all the candidate isotopes for  $0\nu\beta\beta$  decay, NUMEN is conceived in a long-range time perspective. The main experimental tools for this project are the K800 Superconducting Cyclotron and the MAGNEX magnetic spectrometer at the INFN-LNS laboratory in Catania, Italy. In the pilot phase, NUMEN demonstrated the capability of measuring small cross sections in a high background of other reaction channels, with the current experimental setup and in synergy with the ERC NURE project [27]. However, a systematic search on all  $0\nu\beta\beta$  candidate isotopes, with high-precision measurements, is required to achieve the ambitious goal of constraining the NMEs. The small values of DCE cross sections, the resolution, and the sensitivity requirements demand beam intensities much higher than those deliverable with the present facility.

The NUMEN Holy Grail is to study if the DCE cross section, and consequently the DCE NME, is connected to  $0\nu\beta\beta$  NMEs as a smooth function of incident beam energy and target mass. This goal requires the development of the reaction and nuclear structure theory and a systematic set of data. The other NUMEN goals are to provide a new generation of DCE reaction cross-section data to constrain the  $0\nu\beta\beta$  NME theoretical calculations, which is achievable in the short term with a reduced dataset, and to provide relative NME information on the different candidate isotopes for  $0\nu\beta\beta$  decay. The ratio of the DCE cross section can be regarded as a model independent way to compare the sensitivity of  $0\nu\beta\beta$  decay experiments using different isotopes.

To achieve these goals, the project promotes a specific R&D activity with the upgrade of the whole INFN-LNS research infrastructure. In this context, the three-year upgrade project POTLNS (PIR01\_00005) for the production of high-intensity beams has been selected in a national competitive program (PON-MIUR) and has already started the activities.

Investigation of rare processes is the challenge of neutrinoless double-beta decay and of the NUMEN project. Low-background and high-sensitivity detectors are required to search for such rare signals and to give fundamental information to solve the puzzle concerning the neutrino nature.

In the following, the NUMEN tools and strategies will be described, with a focus on the superconducting cyclotron (CS) facility upgrade, in the framework of the POTLNS project, and on the future experiments with high-intensity beams.

## 2. NUMEN Methods and Tools

### 2.1. NUMEN Experimental Methods

The NUMEN idea is to use heavy-ion double-charge exchange (DCE) reactions to simulate the nuclear transition, ground state to ground state, occurring in  $0\nu\beta\beta$  decay. As already mentioned, the two processes, DCE and  $0\nu\beta\beta$ , present many similarities in spite of being mediated by different interactions.

Two main classes of experiments at different energies are foreseen within NUMEN that are meant to probe two isospin directions: lowering  $\tau-\tau-$  and rising  $\tau+\tau+$ . These isospin directions are characteristic of  $\beta-\beta-$  and  $\beta+\beta+$  decays, respectively. The measurements of both  $\beta-\beta-$  and  $\beta+\beta+$  reactions provide a useful test of the procedure to extract NMEs from the measured DCE cross section because NMEs are invariant quantities and so are common to DCE and to its inverse.

In particular, an  $^{18}\text{O}^{8+}$  beam is used to investigate the  $\beta+\beta+$  direction in the target and to measure the  $(^{18}\text{O},^{18}\text{Ne})$  DCE transitions, together with other reaction channels involving the same beam and target. In the same way, a  $^{20}\text{Ne}^{10+}$  beam is used to explore the  $\beta-\beta-$  direction via the  $(^{20}\text{Ne},^{20}\text{O})$  reaction. For each system, target–projectile, the measurements of the DCE reaction, the single-charge exchange reaction, 2p- and 1p-transfer, 2n- and 1n-transfer, and elastic and inelastic scattering are foreseen.

The exploration of these two classes of experiments has already been performed on a few selected isotopes in the last few years [28,29]. The target isotopes, with the technical characteristics for target production, were chosen from among those of interest to the neutrino community with the technologies currently available. The choice of target isotopes is due to a compromise between the interest of the  $0\nu\beta\beta$  scientific community in specific isotopes and the related technical issues. Specifically, the possibility to separate ground state (g.s.)-to-g.s. transition in the DCE-measured energy spectra and the availability of a thin, uniform target of isotopically enriched material were considered. In particular, the  $^{116}\text{Sn}$ ,  $^{76}\text{Se}$ ,  $^{40}\text{Ca}$ , and  $^{48}\text{Ti}$  targets were studied with  $^{18}\text{O}^{8+}$  beams and the  $^{116}\text{Cd}$ ,  $^{130}\text{Te}$ , and  $^{76}\text{Ge}$  targets with  $^{20}\text{Ne}^{10+}$  beams. For each configuration, measurements were carried out using a DCE reaction, an SCE reaction, 2p-transfer, 1p-transfer, 2n-transfer, 1n-transfer, and elastic and inelastic scattering.

The analysis of elastic and inelastic scattering data turned out to be a powerful tool to explore the initial- and final-state interactions in heavy-ion nuclear reactions at high transferred momenta, as has been shown in  $^{76}\text{Ge}-^{76}\text{Se}$  [30–32] and in other systems [33]. In the  $^{116}\text{Cd}(^{20}\text{Ne},^{22}\text{Ne})^{114}\text{Cd}$  two-neutron pickup and  $^{116}\text{Cd}(^{20}\text{Ne},^{18}\text{O})^{118}\text{Sn}$  two-proton stripping reactions at 306 MeV incident energy, selected transitions to low-lying  $0+$  and  $2+$  states of the residual nuclei were analyzed. The role of the couplings with inelastic transitions has been determined [34].

Furthermore, crucial experimental issues need to be addressed in order to measure heavy-ion-induced DCE reactions in both classes of experiments. The main technological challenges are the discrimination among the transitions to individual states and the exploration of a wide momentum transfer range. It is, therefore, necessary to detect heavy ions with good isotope separation and energetic resolution in a wide angular range, including zero degree. Furthermore, measuring the rather small DCE cross sections (down to a few nb) requires considerable rejection efficiency against background events, that is, a remarkably high experimental sensitivity. Background events may be generated by competing reaction processes that, due to the small DCE cross sections, are much more probable to occur. For this reason, a prerequisite for the experiment is high-resolution particle identification. A quantitative method was developed to estimate the particle identification ability and background contamination, which limit the overall sensitivity to the energy spectra [35]. Such analysis was applied for the first time to the  $^{116}\text{Cd}(^{20}\text{Ne},^{20}\text{O})^{116}\text{Sn}$  reaction at 15 AMeV to deduce the absolute cross-section sensitivity of the MAGNEX spectrometer. Other data analyses of the reactions mentioned above are underway.

The NUMEN future phase will consist of a series of experimental campaigns using  $^{18}\text{O}$  and  $^{20}\text{Ne}$  beams of high intensities (some  $\mu\text{A}$ ) and integrated charge of hundreds of mC up to C, for experiments in which coincidence measurements are required, spanning all the variety of  $0\nu\beta\beta$  decay candidate isotopes of interest, like  $^{48}\text{Ca}$ ,  $^{76}\text{Ge}$ ,  $^{76}\text{Se}$ ,  $^{82}\text{Se}$ ,  $^{96}\text{Zr}$ ,  $^{100}\text{Mo}$ ,  $^{106}\text{Cd}$ ,  $^{110}\text{Pd}$ ,  $^{116}\text{Cd}$ ,  $^{110}\text{Sn}$ ,  $^{124}\text{Sn}$ ,  $^{128}\text{Te}$ ,  $^{130}\text{Te}$ ,  $^{136}\text{Xe}$ ,  $^{130}\text{Xe}$ ,  $^{148}\text{Nd}$ ,  $^{150}\text{Nd}$ ,  $^{154}\text{Sm}$ ,  $^{160}\text{Gd}$ , and  $^{198}\text{Pt}$ .

## 2.2. NUMEN Experimental Tools

The main experimental tools for this project are the K800 Superconducting Cyclotron and the MAGNEX (Figure 1) spectrometer at the INFN-LNS laboratory in Catania, Italy.

The K800 Superconducting Cyclotron (CS) is a compact three-sector accelerator capable of delivering ion beams from protons to uranium at energies up to 80 AMeV [36]. The pole has a 90-cm radius, and the internal magnetic field can reach a value of 4.8 T. To achieve such intense magnetic fields, the superconducting cyclotron is equipped with

two pairs of superconductive Nb–Ti coils ( $\alpha$  and  $\beta$ ) immersed in a liquid helium bath at a working temperature of 4.2 K.

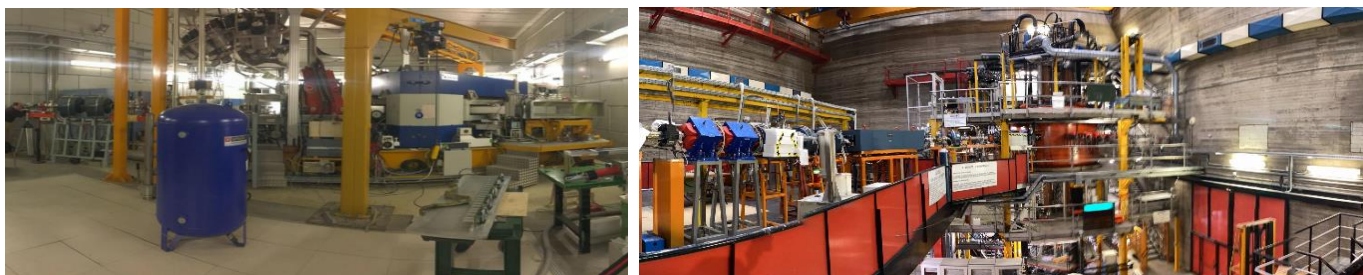


**Figure 1.** Pictures of MAGNEX (left) and of the superconducting cyclotron (CS, right) at the Laboratori Nazionali del Sud.

The 25 years of CS activity show the extremely good versatility and reliability of this accelerator. A broad range of beams could be produced by the K800 CS, allowing hundreds of experiments to be carried out in different fields of scientific and technological research.

MAGNEX [22] is a large acceptance magnetic spectrometer made of a quadrupole with large-aperture vertically focusing and dipole horizontally bending magnets. MAGNEX allows one to identify heavy ions with a good resolution with mass ( $\Delta A/A \sim 1/160$ ), angle ( $\Delta\theta \sim 0.2^\circ$ ), and energy ( $\Delta E/E \sim 1/1000$ ), within a large, solid angle ( $\Omega \sim 50$  msr) and momentum range ( $-14\% < \Delta p/p < +10\%$ ). High-resolution measurements for quasi-elastic processes, characterized by differential cross sections as low as tens of nb/sr, have already been performed by this setup. Significant scientific results have been achieved with MAGNEX in a wide range of masses of the colliding systems and incident energies [37–50], demonstrating the capabilities of this apparatus. The new challenging experimental campaigns with high-intensity beams, foreseen in the NUMEN project, led to intense R&D activity on the detection apparatus, leading to the upgrade of the CS and of the research infrastructures at the LNS, funded by the POTLNS project.

### 2.3. The NUMEN Upgrade

Tiny cross sections and large backgrounds require high-intensity beams and a detection apparatus with high sensitivity. Given these targets, NUMEN supported the POTLNS project, the goal of which is to upgrade the INFN-LNS research infrastructure in order to increase the beam intensity by about 2 orders of magnitude, with respect to the current maximum value, of ion beams with mass numbers less than 40 and energies between 15 and 70 AMeV. The POTLNS project, already started, aims to strengthen those research infrastructures that were identified as a priority in Europe.

The CS currently operates with beam intensities up to a maximum of  $10^{11}$  pps, corresponding to a maximum beam power of the order of 100 W. The intensity necessary for the experiments proposed by NUMEN, and within a reasonable beam time, is about 100 times greater than the current values: thus, intensities of about  $10^{13}$  pps for a maximum power of 10 kW are needed. Consequently, numerous components of the particle accelerator and of the experimental setups must be upgraded in view of the high-intensity operations.

The NUMEN R&D activity has led to technological developments in various fields. For example, the search for new radiation-hard detectors led to the development of silicon carbide (SiC) detectors in the SiCILIA project [51]. The major upgrade of MAGNEX is related to a new focal plane detector (capable of working at rates from a few kHz to several MHz), made of a new gas tracker based on multiple-thick GEM technology, a new SiC–CsI telescope wall for particle identification, and a new array of scintillators, called G-NUMEN [52], for  $\gamma$ -ray measurement in coincidence with MAGNEX. In addition, new electronics, based on the CAEN VX2740 digitizer, and radiation-tolerant isotopically enriched thick targets, with substrates of highly oriented pyrolytic graphite (HOPG), are foreseen [53–56]. A general description of the NUMEN new experimental apparatus, under construction, can be found in [57].

#### 2.4. The NUMEN Particle Accelerator: The LNS Superconducting Cyclotron Upgrade

The experimental campaigns of NUMEN will mainly require beams of carbon, oxygen, and neon with intensities up to  $10^{13}$  pps. The energies required are in the 15–70 AMeV range and the beam power in the 1–10 kW range. The ongoing upgrade of the INFN-LNS facilities in the framework of the POTLNS project also includes new MAGNEX power supplies in order to increase the maximum magnetic rigidity acceptance from 1.8 Tm to 2.2 Tm. In fact, the best compromise to overcome the current limit of 1.8 Tm is to maintain the present configuration of the dipole magnet and to increase the current by enhancing the dipole power supplies and, consequently, the water-cooling system.

A new beam extraction method based on a stripping foil will be used to address the requirement to enhance the maximum CS accelerator beam power current. The usage of the present electrostatic extraction method is not feasible due to its low efficiency.

Furthermore, due to the small transverse dimensions of the existing extraction channel and the lack of thermal shields to dissipate the power of the beam from the halos of the beam itself, the CS will be upgraded with a new extraction channel specifically designed for stripping extraction [58–61]. To allow for stripping extraction, ions are accelerated with a charge state  $q = (Z-2) \div (Z-5)$  and then get fully stripped by crossing a stripper foil. The use of a stripper foil, placed in a proper position near the maximum radius, allows the beam trajectories to escape from the region of the cyclotron pole. All the ions of interest, with mass  $\leq 40$  a.m.u. and energy  $\geq 15$  AMeV, are fully stripped with efficiency higher than 99% [62]. Beam power losses inside the cyclotron are designed to be below 100–200 W, which is a reasonable value as far as activation is concerned.

Beam dynamics is crucial for extraction by stripping because the axial and radial envelopes have to be kept as small as possible along the entire extraction path, from the stripper to the exit of the cyclotron, although the trajectories cross the hill boundaries at different angles for each trajectory. The number of correction elements to be used along the new extraction channel has to be minimized, and the extraction channel design has to be done carefully. A detailed beam dynamics study [59–61] demonstrated that, with the proper design of the stripper foil system [63], it is possible to make the trajectories of the beams cross at the same exit point. Moreover, since extraction by stripping is a multi-turn extraction, it is mandatory to consider in the simulations the value of energy spread after the crossing of the stripping foil in order to evaluate correctly the radial beam size. According to [64], and as confirmed by our dedicated simulations, the energy spread at the exit point of the accelerator is expected to be below  $\pm 0.3\%$  [65] for all ions and energies. A new exit beam transport line has been designed to match the new extraction channel to the existing transport line at the magnet EXDP01. This line is designed to compensate for the chromaticity of the extraction path so as to produce an achromatic beam waist.

The new beam transport line of the LNS is shown in Figure 2. In particular, the beam is handled by the fragment ion separator (FRAISE) line [66] before reaching the MAGNEX room. FRAISE is designed for the production and separation of radioactive ion beams. The beam strikes the production target, where about 10–15% of the power is dissipated, while most of the beam is stopped in the vacuum chamber of the dipole FSDP01. The FRAISE room allows working with primary beam power up to 3 kW, when the beam has to be stopped there. For this reason, the FRAISE room is the appropriate place where to tailor the beam characteristics to match the requirements of the NUMEN experiments. The NUMEN experiments require a beam spot on the target with a horizontal size of 1 mm, horizontal divergence of 8 mrad, and energy spread of 0.1% (all these values are FWHM). These characteristics are still quite far from being met by the beam extracted from the cyclotron. For these reasons, the beam structure must be reshaped in terms of dimensions and divergences by cutting the beam halo in horizontal and vertical planes and, then, by reducing the beam emittance.

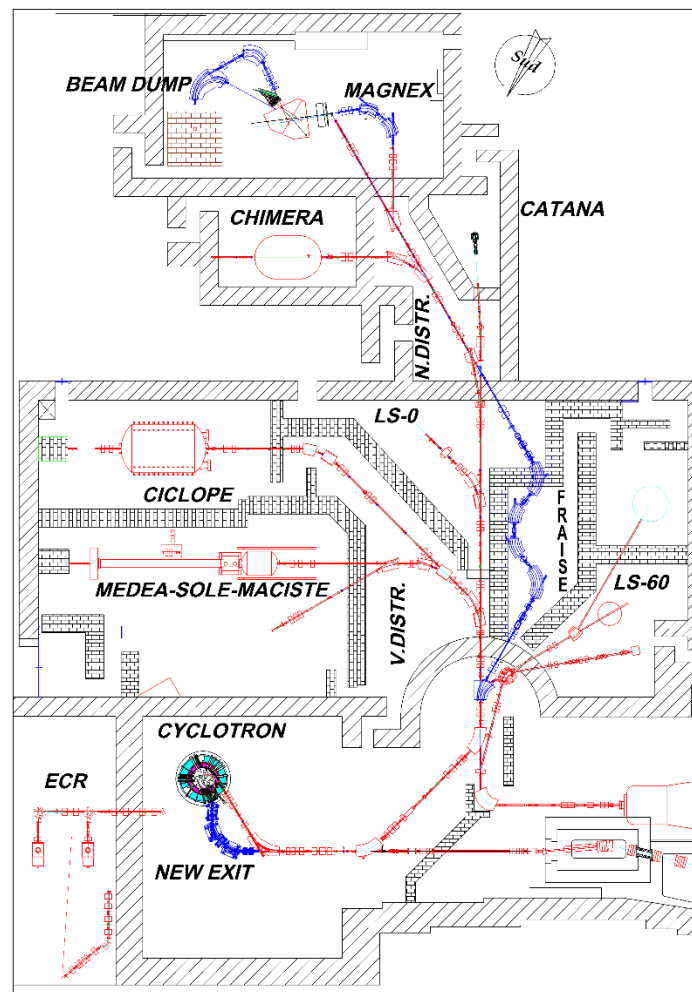


**Figure 2.** New layout of the LNS. From the CS the beams reach the MAGNEX area through the fragment ion separator (FRAISE) line. The experimental MAGNEX area has to be modified to host a large beam dump.

The energy beam spread can also be reduced by using the dispersion properties of the FRAISE beam line. The horizontal size can be strongly reduced at the designed target position for the production of a radioactive beam of FRAISE. Here, the beam can be strongly focused and the beam tail exceeding the dimension of 1 mm horizontally and 1.6 mm vertically can be intercepted by an appropriately cooled collimator/slits. Additional collimators will be installed just before the quadrupole FSQP03 and FSQP04 to define the horizontal and vertical divergence, respectively. To mitigate the heating of these collimators, their thickness is chosen to reduce the energy of the particles crossing through them to 10–20% only. Indeed, the energy lost through the collimators allows the first dipole FSDP01 of the FRAISE line to bend these particles on the inner side of its vacuum chamber, designed to stop beam power up to 4 kW. To reduce the intrinsic energy spread of the beams extracted by stripping from the expected value of 0.3% FWHM down to 0.1% FWHM, two options are under investigation. The first option is based on the use of the high dispersive properties of the FRAISE line at the symmetry plane (25 mm of radial dispersion for an energy spread of 1%) and selection of the energy spread using collimators/slits. Another, more elegant, solution is to use a well-shaped wedged degrader that, according our preliminary simulations, could reduce the energy spread below the target value of 0.1%. This latter option is very appealing, and we are evaluating and simulating the effect of the increase on the final size of and divergence in the horizontal plane. The final solution adopted to minimize the beam losses and to meet the limits of beam power loss along

the different areas of the beam transport line will likely consist in a combination of all these methods.

Extraction by stripping of beams with power up to 10 kW needs an acceleration chamber with a larger vertical gap inside the cyclotron in order to minimize the beam losses and to have better vacuum conductance. In our project, the vertical gap in the pole region will be increased from the current value of 24 mm to 30 mm. This will be achieved by replacing the existing liners with new, thinner ones. The results of the beam dynamics study also show that it is mandatory to have a new extraction channel in the cryostat of the cyclotron with a different direction and larger clearance both in radial and vertical directions with respect to the existing extraction channel. Therefore, the present cryostat has to be replaced with a new one [67].

New technologies will be used to build the new superconducting coils that, using smaller coils with a higher current density, achieve the same performance. In this way, the cryostat design is simplified and the consumption of cryogenic liquids such as liquid helium and liquid nitrogen is reduced. The smaller size of the new coils also allows increasing the vertical gap in the extraction channel up to 60.5 mm versus the present value of 30.5 mm. This wider clearance makes the insertion of the magnetic channels easier: they are additional iron elements, placed outside the pole radius, that change locally the magnetic field, help radial focusing, and slightly steer the beam when necessary [68–70].

The design of the new penetrations and subsystems was conceived to avoid mechanical interference with the existing ones since the extraction of the other ions of the CS operating scheme by the deflector will be maintained anyhow.

### 2.5. The New Beam Lines inside the MAGNEX Hall

The new beam line to transport the beam to the MAGNEX spectrometer has already been designed, and it is shown in Figure 3. It consists of the existing quadrupole triplet, also called the TEBE line, and of two new dipoles and three new quadrupoles, to be installed. The two dipoles, MADP01 and MADP02, are equal and have a bending angle of  $47.5^\circ$ . The characteristics of the last two quadrupoles were optimized to keep a distance of at least 700 mm between the end of the last quadrupole and the target, while the quadrupole between the two dipoles, MADP01 and MADP02, is an existing one of the LNS.

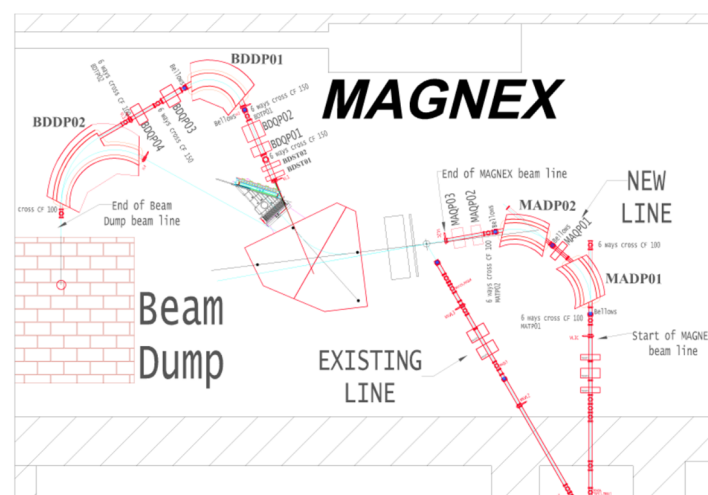


**Figure 3.** Layout of the new MAGNEX experimental area.

The beam envelope along the beam transport line from the FRAISE exit to the NUMEN target is shown in Figure 4. The new beam line inside the MAGNEX experimental area is shown in Figure 5. According to the requirements of the experiment, the beam spot on the target has the following size:  $x = 1$  mm and  $y = 2.5$  mm FWHM. The divergences are below the values of 8.5 mrad and 15 mrad FWHM in the horizontal and vertical directions,

respectively. To achieve this goal, the geometrical emittances of the beam have to be properly shaped along the FRAISE line and the energy spread has to be reduced to the target value of 0.1% FWHM.

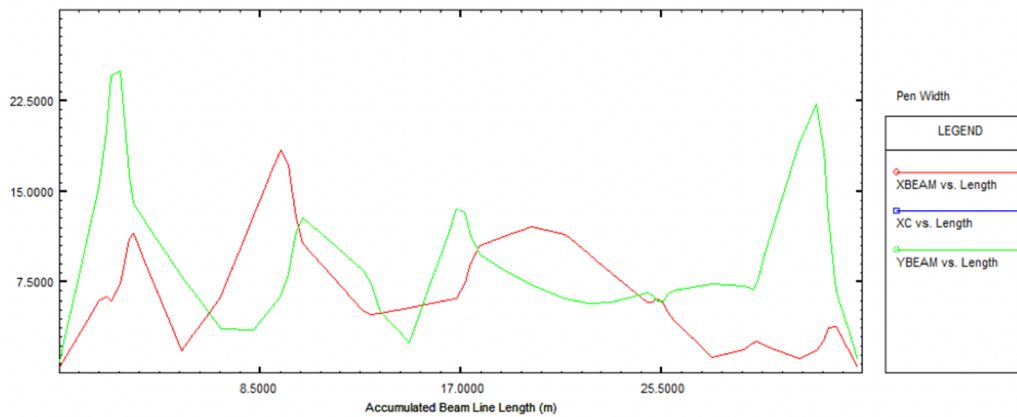


**Figure 4.** Beam envelope (mm) as a function of the transport beam line length (m) from the end of the FRAISE line to the NUMEN target.

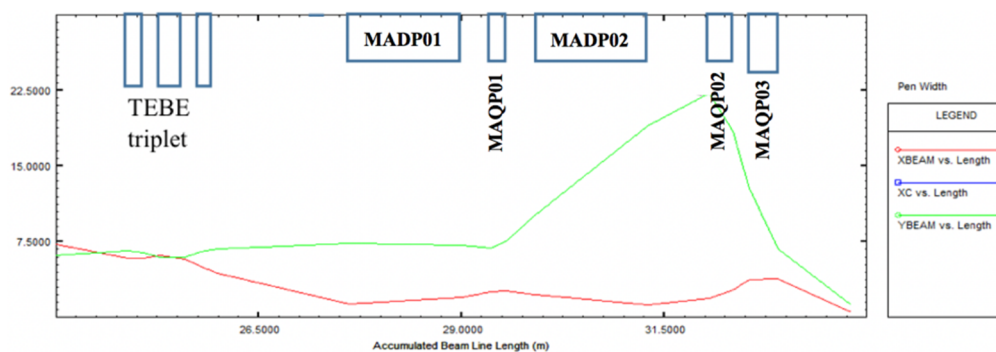


**Figure 5.** Beam envelope (mm) as a function of the transport beam line length (m) inside the MAGNEX area.

The diameters of the vacuum chamber of the three quadrupoles of the two dipoles of the new beam line are quite large with respect to the beam envelope across each element. All quadrupole magnets have a pole diameter of 70 mm, but MAQP01 has a pole diameter of 80 mm. Similarly, the vacuum gap of the two big dipoles is 66 mm. These constraints were set in order to minimize the risk of beam losses through these elements and consequently to minimize the background in the MAGNEX focal plane detector.

A key issue for the NUMEN experiments is to transport the beam coming from the target up to a well-shielded beam dump. Moreover, MAGNEX will be operated in two different positions, of  $+3^\circ$  or  $-3^\circ$  vs. the incident beam direction, so to allow for the detection of the reaction products with magnetic rigidity lower or higher than that of the incident beam, respectively. This means that two different beam lines are needed to transport the beam from MAGNEX to the beam dump. To minimize the cost of the two beam lines, the first half of these two lines was designed to have the same magnetic elements with the same characteristics. Moreover, in order to leave enough room around the detector of MAGNEX, we decided to move the first part of the exit line from the left-side to the right-side exit ( $+3^\circ$  or  $-3^\circ$ ), or vice versa, according to the experimental configuration. Consequently, it will be necessary to dismount this beam line section, about 3 m long, consisting of two steerer magnets and two big quadrupoles, and to move it from the left side to the right side of the new MAGNEX exit. All the other devices of the two exit beam lines do not need to be moved.

The production of high intensity beams also implies the development of control systems equipped with intelligent sensors of high sensitivity connected in real time, adequate to trigger immediate intervention in case of failure of the beam transport systems. Therefore, smart sensor networks and integration technologies will be developed and tested. To speed up and optimize the transport of the beams, thus making it safer, new software will also be continuously developed with the ability to learn and process the signals obtained from the sensor networks that can then have applications in various other fields, such as environmental monitoring.

## 2.6. The New Beam Dump

The new beam dump, to be placed in the MAGNEX experimental hall, has to handle a power up to 10 kW and must have enough shielding to reduce significantly the background in the MAGNEX focal plane detector due to the neutron and gamma radiation produced by the interaction of the beam with the cooled target of the beam dump.

The beam dump is shielded by a concrete box with both lateral sides of 4.5 m and a height of 4 m. The installation of such a massive beam dump in the MAGNEX experimental room is not an easy task, and many solutions were investigated before the final choice, presented in Figure 6. One of the main issues in selecting the position of the beam dump inside the MAGNEX area is related to the feature of the NUMEN experiment to detect particles that have magnetic rigidity lower or higher than that of the incident beam.

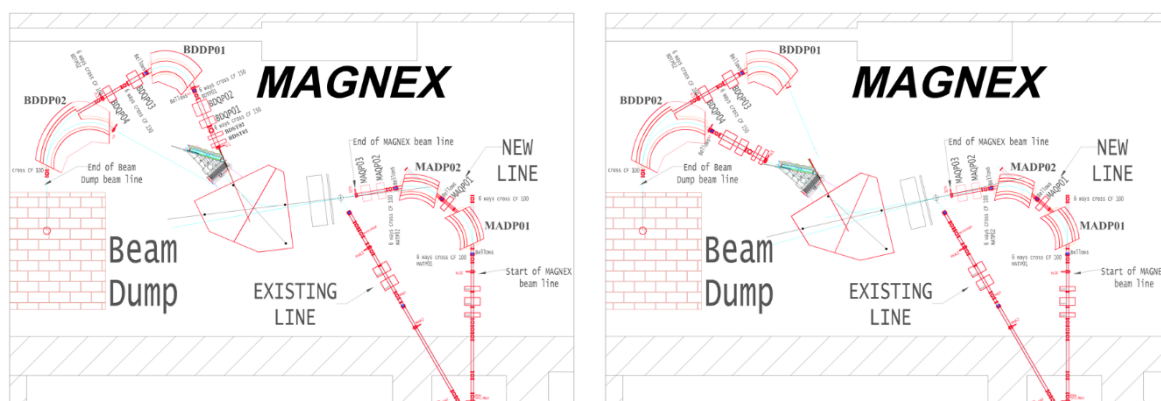


**Figure 6.** The two figures show the different MAGNEX positions, on the left the  $-3^\circ$  position and on the right the  $+3^\circ$  position with respect to the new MAGNEX beam line. In the main layout of the new MAGNEX experimental area, the wall on the left side will be moved by about 4.5 m to allow the installation of the large beam dump. The MAGNEX spectrometer will be rotated by  $70^\circ$  with respect to its actual  $0^\circ$  position to allow the transport of the beam coming from the spectrometer to be transported to the beam dump. A new line is necessary to deliver the beam to the MAGNEX at the new position.

To meet this requirement, the incident beam has to leave the MAGNEX spectrometer through two possible exit ways, one on the left of the focal plane detector (MAGNEX rotated by  $+3^\circ$  with respect to the incident beam) and another on the right (MAGNEX rotated by  $-3^\circ$  with respect to the incident beam); see Figure 6. The left exit or the right exit is used in the case to detect particles that have magnetic rigidity lower or higher than that of the incident beam, respectively.

To host this large beam dump, the MAGNEX room has to be enlarged by about 4 m on the left side and the spectrometer has to be rotated by  $70^\circ$  with respect to its original position. As a consequence, the installation of a new beam line at the entrance of the spectrometer is also needed; see Figure 6.

## 3. NUMEN Strategy for Experiments with High-Intensity Beams

A careful data taking strategy is mandatory to avoid fast and unsustainable saturation of the throughput and of the data storage volume. The first experimental configuration of NUMEN runs will be devoted to the study of the double-charge exchange (DCE) ground-

state-to-ground-state (g.s.-to-g.s.) transitions in conditions where the ground-state peak can be well isolated by MAGNEX inclusive measurements. The beam current for this mode will be the maximum one ( $\sim 10^{13}$  pps). The MAGNEX focal plane detector (FPD) acceptance will be reduced to 10% by exploring only the ground-state region. No gamma array detector will be used. The expected data throughput will be about 60 MB/sec, corresponding to  $\sim 5$  TB/day. During a NUMEN run, other than DCE g.s. transition, several other reaction channels (single-charge exchange, multi-nucleon transfer, elastic and inelastic) are also measured and an extended energy spectrum of the DCE up to large excitation energy is obtained. However, since all other reactions (other than DCE g.s.) are characterized by much larger cross sections, it is not necessary to use a full-power beam. In these studies, the MAGNEX FPD will work in full (100%) momentum acceptance and coincidence with gamma array is typically not needed. The expected data throughput will be about 6 MB/sec, corresponding to  $\sim 0.5$  TB/day.

In many experimental conditions, the DCE g.s.-to-g.s. transition is not well isolated by using MAGNEX alone and measurements of the  $\gamma$  decay of the first excited states with the G-NUMEN [52] array are needed. In these cases, the beam current should be kept at  $\sim 10^{12}$  pps in order to limit the average reactions occurring at the target per beam bunch to about 1, thus keeping the best observational limit for DCE g.s. The  $\gamma$  spectra will be gated in the energy region of interest. The MAGNEX FPD momentum acceptance will be reduced to 10%, measured only in the g.s. region. Under these conditions, the data throughput would be  $\sim 60$  MB/s, corresponding to  $\sim 5$  TB/day.

The typical experiment duration will be of the order of 30 days, producing data storage of 140 TB, which is affordable. About  $10^3$  DCE g.s. coincidence events are expected after proper analysis.

For all the isotope candidates for  $0\nu\beta\beta$  decay, like  $^{48}\text{Ca}$ ,  $^{76}\text{Ge}$ ,  $^{76}\text{Se}$ ,  $^{82}\text{Se}$ ,  $^{96}\text{Zr}$ ,  $^{100}\text{Mo}$ ,  $^{106}\text{Cd}$ ,  $^{110}\text{Pd}$ ,  $^{116}\text{Cd}$ ,  $^{110}\text{Sn}$ ,  $^{124}\text{Sn}$ ,  $^{128}\text{Te}$ ,  $^{130}\text{Te}$ ,  $^{136}\text{Xe}$ ,  $^{130}\text{Xe}$ ,  $^{148}\text{Nd}$ ,  $^{150}\text{Nd}$ ,  $^{154}\text{Sm}$ ,  $^{160}\text{Gd}$ , and  $^{198}\text{Pt}$ , for the experiments in which  $\gamma$  coincidence measurements are required, NUMEN experimental campaigns at high beam intensities (some  $\mu\text{A}$ ) and integrated charge of hundreds of mC up to C are foreseen. The experiments will be performed at different incident energies in order to study the reaction mechanism and, in particular, to explore the dependence on energy of the different spin–isospin components of the nucleon–nucleon interaction and identify the Fermi, Gamow–Teller (GT), and tensor components in the nuclear matrix elements.

#### 4. Discussion

To achieve the ambitious scientific goals of NUMEN, a wide dataset of DCE data is necessary, with systematic exploration of all the cases of interest for  $0\nu\beta\beta$  decay, including data at different bombarding energies and with several isotopic targets. The DCE reaction process needs to be described in detail to identify the relevant nuclear response from the measured DCE cross sections, which is by itself an interesting research goal for nuclear reaction theory. DCE NMEs can be inferred by measured cross sections under controlled laboratory conditions and can be connected to NMEs relevant for  $0\nu\beta\beta$  decay [71]. The analysis of the net of direct quasi-elastic reactions occurring in the projectile-target collision can provide additional information on the nuclear response of  $0\nu\beta\beta$  decay candidate nuclei since they probe selected degrees of freedom of the nuclear structure [72,73]. DCE cross sections can be studied within the same overall reaction coupling scheme. Different reaction mechanisms potentially contribute; among these, the Majorana mechanism is a very promising source of information on the actual nuclear response relevant for  $0\nu\beta\beta$  decay [74]. Nuclear structure models combined with reaction theory and confronted with measured observables will give rise to constrained theories to be adopted for the determination of  $0\nu\beta\beta$  decay NMEs.

Given these considerations, it is mandatory to perform DCE experiments with much higher beam intensities than currently possible, such as those available after the upgrade of the LNS in the framework of the POTLNS project. Strategies for carrying out new NUMEN

experiments with high-intensity beams have been developed to obtain the statistics and the sensitivity necessary to meet the challenge of providing experimental constraints to  $0\nu\beta\beta$  NMEs. The experiments will be performed at different incident energies in order to study the reaction mechanism and, in particular, to explore the dependence on energy of the different spin–isospin components of the nucleon–nucleon interaction and identify the Fermi, GT, and tensor components in the nuclear matrix elements.

**Author Contributions:** Writing and draft preparation, C.A.; spokespersons responsible for the whole NUMEN project, C.A. and F.C.; CS upgrade and new beam line study and design, A.D.R.; beam line upgrade, L.C. (Luciano Calabretta), in collaboration with A.D.R., G.D., and L.C. (Luigi Campajola); EU ERC project NURE, Principal Investigator of ERC NURE is referred to M.C.; MAGNEX experiments, M.C.; data reduction and PID, D.C. (Diana Carbone); tracker, D.T.; front-end-readout electronics and data acquisition, P.F.; DAQ, computation, and simulations, L.P.; integration, D.C. (Daniela Calvo), in collaboration with D.S.; development of radiation-tolerant targets, F.I., in collaboration with V.C. and F.P. All authors have read and agreed to the published version of the manuscript.

**Funding:** The NUMEN project is mainly funded by INFN. Additional funds came from the Italian Ministry of University and Research under the national PON program, with grant number PIR01\_00005 and acronym POTLNS. This work has received funding also from the European Research Council (ERC) under the European Union’s Horizon 2020 research and innovation program, NURE project, grant agreement no. 714625.

**Acknowledgments:** The authors would like to thank the whole staff of the LNS Accelerator Division for the constant support provided.

**Conflicts of Interest:** The authors declare no conflict of interest. The funders had no role in the design of the study; in the collection, analyses, or interpretation of data; in the writing of the manuscript; or in the decision to publish the results.

## References

1. Furry, W.H. On Transition Probabilities in Double Beta-Disintegration. *Phys. Rev.* **1939**, *56*, 1184–1193. [[CrossRef](#)]
2. Goeppert-Mayer, M. Double Beta-Disintegration. *Phys. Rev.* **1935**, *48*, 512–516. [[CrossRef](#)]
3. Majorana, E. Theory of the Symmetry of Electrons and Positrons. *Nuovo Cim.* **1937**, *14*, 171–184. [[CrossRef](#)]
4. Alduino, C.; Alfonso, K.; Avignone, F.T., III; Azzolini, O.; Bari, G.; Bellini, F.; Benato, G.; Bersani, A.; Biassoni, M.; Branca, A.; et al. (CUORE Collaboration) First results of CUORE experiment. *J. Phys. Conf. Ser.* **2020**, *1342*, 012002. [[CrossRef](#)]
5. Kermaidic, Y. GERDA, MAJORANA and LEGEND collaboration GERDA, Majorana and LEGEND towards a background free ton-scale Ge76 experiment. *Proc. Neutrino* **2020**, *2020*. [[CrossRef](#)]
6. Albert, J.B.; Anton, G.; Badhrees, I.; Barbeau, P.S.; Bayerlein, R.; Beck, D.; Belov, V.; Breidenbach, M.; Brunner, T.; Cao, G.F.; et al. (The EXO-200 collaboration); Search for neutrinoless double beta decay with the upgraded EXO-200 detector. *Phys. Rev. Lett.* **2018**, *120*, 07270. [[CrossRef](#)]
7. Gando, A.; Gando, Y.; Hachiya, T.; Hayashi, A.; Hayashida, S.; Ikeda, H.; Inoue, K.; Ishidoshiro, K.; Karino, Y.; Koga, M.; et al. (KamLAND-Zen Collaboration) Search for Majorana Neutrinos Near the Inverted Mass Hierarchy Region with Kam. I. LAND-Zen. *Phys. Rev. Lett.* **2016**, *117*, 082503. [[CrossRef](#)]
8. Iida, T.; Kishimoto, T.; Nomachi, M.; Ajimura, S.; Umehara, S.; Nakajima, K.; Ichimura, K.; Yoshida, S.; Suzuki, K.; Kakubata, H.; et al. The CANDLES experiment for the study of Ca-48 double beta decay. *Nucl. Part. Phys. Proc.* **2016**, *273–275*, 2633–2635. [[CrossRef](#)]
9. Anderson, M.; Andringa, S.; Arushanova, E.; Asahi, S.; Askins, M.; Auty, D.J.; Back, A.R.; Barnard, Z.; Barros, N.; Bartlett, D.; et al. Search for invisible modes of nucleon decay in water with the SNO+ detector. *Phys. Rev. D* **2019**, *99*, 032008. [[CrossRef](#)]
10. Alenkov, V.; Bae, H.W.; Beyer, J.; Boiko, R.S.; Boonin, K.; Buzanov, O.; Chanthima, N.; Cheoun, M.K.; Chernyak, D.M.; Cho, J.S.; et al. First results from the AMoRE-Pilot neutrinoless double beta decay experiment. *Eur. Phys. J. C* **2019**, *79*, 791. [[CrossRef](#)]
11. Barabash, A.S.; Basharina-Freshville, A.; Blot, S.; Bongrand, M.; Bourgeois, C.; Breto, D.; Brudanin, V.; Buresova, H.; Busto, J.; Caffrey, A.J.; et al. Calorimeter development for the SuperNEMO double beta decay experiment. *Nucl. Inst. Methods Phys. Res. A* **2017**, *868*, 98–108. [[CrossRef](#)]
12. Ejiri, H.; Suhonen, J.; Zuber, K. Neutrino nuclear responses for astro-neutrinos, single-decays and double beta decays. *Phys. Rep.* **2019**, *797*, 1. [[CrossRef](#)]
13. Ejiri, H. Neutrino-Mass Sensitivity and Nuclear Matrix Element for Neutrinoless Double Beta Decay. *Universe* **2020**, *6*, 225. [[CrossRef](#)]
14. Vergados, D.; Ejiri, H.; Simkovic, F. Theory of neutrinoless double beta decay. *Rep. Prog. Phys.* **2012**, *75*, 106301. [[CrossRef](#)]
15. Gouvea, A.; Vogel, P. Lepton flavor and number conservation, and physics beyond the standard model. *Prog. Part. Nucl. Phys.* **2013**, *71*, 75. [[CrossRef](#)]
16. Suhonen, J.; Civitarese, O. Review of the properties of the  $0\nu\beta\beta$  nuclear matrix elements. *J. Phys. G* **2012**, *39*, 124005. [[CrossRef](#)]

17. Barea, J.; Kotila, J.; Iachello, F. Nuclear matrix elements for double- $\beta$  decay. *Phys. Rev. C* **2013**, *87*, 014315. [[CrossRef](#)]
18. DellOro, S.; Marcocci, S.; Viel, M.; Vissani, F. Neutrinoless double beta decay: 2015 review. *Adv. High Energy Phys.* **2016**, *2016*, 2162659. [[CrossRef](#)]
19. Agodi, C.; Cappuzzello, F.; Cavallaro, M.; Bondi, M.; Carbone, D.; Cunsolo, A.; Foti, A. Heavy 1 ions double charge exchange reactions: Towards the 0 nuclear matrix element determination. *Nucl. Part. Physics Proc.* **2015**, *265–266*, 28–30. [[CrossRef](#)]
20. Cappuzzello, F.; Agodi, C.; Bondi, M.; Carbone, D.; Cavallaro, M.; Foti, A. The role of nuclear reactions in the problem of 0 decay and the NUMEN project at INFN-LNS. *J. Phys. Conf. Ser.* **2015**, *630*, 012018. [[CrossRef](#)]
21. Cappuzzello, F.; Agodi, C.; Cavallaro, M.; Carbone, D.; Tudisco, S.; Presti, D.L.; Oliveira, J.R.B.; Finocchiaro, P.; Colonna, M.; Rifuggiato, D.; et al. The NUMEN project: NUclear Matrix Elements for Neutrinoless double beta decay. *Eur. Phys. J. A* **2018**, *54*, 72. [[CrossRef](#)]
22. Cappuzzello, F.; Cavallaro, M.; Agodi, C.; Bondi, M.; Carbone, D.; Cunsolo, A.; Foti, A. Heavy-ion double charge exchange reactions: A tool toward  $0\nu\beta\beta$  nuclear matrix element. *Eur. Phys. J. A* **2015**, *51*, 145. [[CrossRef](#)]
23. Cappuzzello, F.; Agodi, C.; Carbone, D.; Cavallaro, M. The MAGNEX spectrometer: Results and perspectives. *Eur. Phys. J. A* **2016**, *52*, 1–44. [[CrossRef](#)]
24. Lenske, H.; Cappuzzello, F.; Cavallaro, M.; Colonna, M. Heavy ion charge exchange reactions as probes for nuclear  $\beta$ -decay. *Prog. Part. Nucl. Phys.* **2019**, *109*, 103. [[CrossRef](#)]
25. Cappuzzello, F.; Cavallaro, M. Nuclear Response to Second-Order Isospin Probes in Connection to Double Beta Decay. *Universe* **2020**, *6*, 217. [[CrossRef](#)]
26. Suhonen, J.; Civitarese, O. Weak-interaction and nuclear-structure aspects of nuclear double beta decay. *Phys. Rep.* **1998**, *300*, 123–214. [[CrossRef](#)]
27. Ejiri, H.; Hashim, I.H.; Hino, Y.; Kuno, Y.; Matsumoto, Y.; Ninomiya, K.; Sakamoto, H.; Sato, A.; Shima, T.; Shinohara, A.; et al. Nuclear  $\gamma$  Rays from Stopped Muon Capture Reactions for Nuclear Isotope Detection. *J. Phys. Soc. Jpn.* **2013**, *82*, 044202. [[CrossRef](#)]
28. Cavallaro, M.; Aciksoz, E.; Acosta, L.; Agodi, C.; Auerbach, N.; Bellone, J.; Bijker, R.; Bianco, S.; Bonanno, D.; Bongiovanni, D.; et al. NURE: An ERC project to study nuclear reactions for neutrinoless double beta decay. In Proceedings of the Proceedings of 55th International Winter Meeting on Nuclear Physics—PoS(BORMIO2017). *Sissa Medialab. Srl.* **2017**, *302*, 15.
29. Calabrese, S.; Cappuzzello, F.; Carbone, D.; Cavallaro, M.; Agodi, C.; Acosta, L.; Bonanno, D.; Bongiovanni, D.; Borello-Lewin, T.; Boztosun, I.; et al. First measurement of the  $^{116}\text{Cd}(^{20}\text{Ne},^{20}\text{O})^{116}\text{Sn}$  reaction at 15 A MeV. *Acta Phys. Pol.* **2018**, *B 49*, 275. [[CrossRef](#)]
30. Cavallaro, M.; Agodi, C.; Brischetto, G.; Calabrese, S.; Cappuzzello, F.; Carbone, D.; Cirraldo, I.; Pakou, A.; Sgouros, O.; Soukeras, V.; et al. The MAGNEX magnetic spectrometer for double charge exchange reactions. *Nucl. Instrum. Methods Phys. Res. Sect. B Beam Interact. Mater. Atoms* **2020**, *463*, 334–338. [[CrossRef](#)]
31. Spatafora, A.; Cappuzzello, F.; Carbone, D.; Cavallaro, M.; Lay, J.A.; Acosta, L.; Agodi, C.; Bonanno, D.; Bongiovanni, D.; Boztosun, I.G.A.; et al.  $^{20}\text{Ne} + ^{76}\text{Ge}$  elastic and inelastic scattering at 306 mev. *Phys. Rev. C* **2019**, *100*, 034620. [[CrossRef](#)]
32. Cavallaro, M.; Bellone, J.I.; Calabrese, S.; Agodi, C.; Burrello, S.; Cappuzzello, F.; Carbone, D.; Colonna, M.; Deshmukh, N.; Lenske, H.; et al. A constrained analysis of the  $^{40}\text{Ca}(^{18}\text{O},^{18}\text{F})^{40}\text{K}$  direct charge exchange reaction mechanism at 275 MeV. *Front. Astron. Space Sci.* accepted.
33. Carbone, D.; Linares, R.; Amador-Valenzuela, P.; Calabrese, S.; Cappuzzello, F.; Cavallaro, M.; Firat, S.; Fisichella, M.; Spatafora, A.; Acosta, L.; et al. Initial State Interaction for the  $^{20}\text{Ne} + ^{130}\text{Te}$  and  $^{18}\text{O} + ^{116}\text{Sn}$  Systems at 15.3 A MeV from Elastic and Inelastic Scattering Measurements. *Universe* **2021**, *7*, 58. [[CrossRef](#)]
34. Carbone, D.; Ferreira, J.L.; Calabrese, S.; Cappuzzello, F.; Cavallaro, M.; Hacialihoglu, A.; Lenske, H.; Lubian, J.; Vsevolodovna, R.I.M.; Santopinto, E.; et al. Analysis of two-nucleon transfer reactions in the  $^{20}\text{Ne} + ^{116}\text{Cd}$  system at 306 MeV. *Phys. Rev. C* **2020**, *102*, 044606. [[CrossRef](#)]
35. Calabrese, S.; Cappuzzello, F.; Carbone, D.; Cavallaro, M.; Agodi, C.; Torresi, D.; Acosta, L.; Bonanno, D.; Bongiovanni, D.; Borello-Lewin, T.; et al. Analysis of the background on cross section measurements with the MAGNEX spectrometer: The  $(^{20}\text{Ne}, ^{20}\text{O})$  Double Charge Exchange case. *Nucl. Instruments Methods Phys. Res. Sect. A Accel. Spectrometers Detect. Assoc. Equip.* **2020**, *980*, 164500. [[CrossRef](#)]
36. Rifuggiato, D.; Calabretta, L.; Cosentino, L.; Cuttone, G. 2013 Proceedings of Cyclotrons, Vancouver, BC, Canada, JACOW. Available online: <https://accelconf.web.cern.ch/AccelConf/cyclotrons2013/papers/MOPPT011.pdf> (accessed on 16 March 2021).
37. Carbone, D.; Ferreira, J.L.; Cappuzzello, F.; Lubian, J.; Agodi, C.; Cavallaro, M.; Foti, A.; Gargano, A.; Lenzi, S.M.; Linares, R.; et al. Microscopic cluster model for the description of new experimental results on the  $^{13}\text{C}(^{18}\text{O},^{16}\text{O})^{15}\text{C}$  two-neutron transfer at 84 MeV incident energy. *Phys. Rev. C* **2017**, *95*, 034603. [[CrossRef](#)]
38. Cavallaro, M.; Agodi, C.; Assié, M.; Azaiez, F.; Cappuzzello, F.; Carbone, D.; De Séreville, N.; Foti, A.; Pandola, L.; Scarpaci, J.A.; et al. Neutron decay of  $^{15}\text{C}$  resonances by measurements of neutron time-of-flight. *Phys. Rev. C* **2016**, *93*, 064323. [[CrossRef](#)]
39. Ermamatov, M.J.; Cappuzzello, F.; Lubian, J.; Cubero, M.; Agodi, C.; Carbone, D.; Cavallaro, M.; Ferreira, J.L.; Foti, A.; Garcia, V.N.; et al. Two-neutron transfer analysis of the  $^{16}\text{O}(^{18}\text{O},^{16}\text{O})^{18}\text{O}$  reaction. *Phys. Rev. C* **2016**, *94*, 024610. [[CrossRef](#)]
40. Carbone, D.; Cappuzzello, F.; Cavallaro, M.; Cunsolo, A.; Foti, A.; Tudisco, S.; Bondi, M.; Santagati, G.; Taranto, G.; Chen, R.; et al. Enhancement of the two neutron transfer channel in  $^{18}\text{O}$  induced reactions at 84 MeV. *J. Phys. Conf. Ser.* **2011**, *312*, 082016. [[CrossRef](#)]

41. Cappuzzello, F.; Agodi, C.; Bondi, M.; Carbone, D.; Cavallaro, M.; Cunsolo, A.; Napoli, M.D.; Foti, A.; Nicolosi, D.; Tropea, S. A broad angular-range measurement of elastic and inelastic scatterings in the  $^{16}\text{O}$  on  $^{27}\text{Al}$  reaction at 17.5mev/u. *Nucl. Instrum. Methods Phys. Res. Sect. A Accel. Spectrometers Detect. Assoc. Equip.* **2014**, *763*, 314–319. [[CrossRef](#)]
42. Agodi, C.; Giuliani, G.; Cappuzzello, F.; Bonasera, A.; Carbone, D.; Cavallaro, M.; Foti, A.; Linares, R.; Santagati, G. Analysis of pairing correlations in neutron transfer reactions and comparison to the constrained molecular dynamics model. *Phys. Rev. C* **2018**, *97*, 034616. [[CrossRef](#)]
43. Carbone, D.; Bondi, M.; Bonaccorso, A.; Agodi, C.; Cappuzzello, F.; Cavallaro, M.; Charity, R.J.; Cunsolo, A.; de Napoli, M.; Foti, A. First application of then- $^9\text{Be}$  optical potential to the study of the  $^{10}\text{Be}$  continuum via the  $(^{18}\text{O},^{17}\text{O})$  neutron-transfer reaction. *Phys. Rev. C* **2014**, *90*. [[CrossRef](#)]
44. Cappuzzello, F.; Carbone, F.; Cavallaro, D.; Bondi, M.; Agodi, M.; Azaiez, C.; Bonaccorso, F.; Cunsolo, A.; Vitturi, A. Signatures of the Giant Pairing Vibration in the  $^{14}\text{C}$  and  $^{15}\text{C}$  atomic nuclei. *Nat. Commun.* **2015**, *6*, 6743. [[CrossRef](#)] [[PubMed](#)]
45. Paes, B.; Santagati, G.; Magana Vsevolodovna, R.; Cappuzzello, F.; Carbone, D.; Cardozo, E.N.; Cavallaro, M.; García-Tecocoatzi, H.; Gargano, A.; Ferreira, J.L.; et al. Long-range versus short-range correlations in the two-neutron transfer reaction  $^{64}\text{Ni}(^{18}\text{O},^{16}\text{O})^{66}\text{Ni}$ . *Phys. Rev. C* **2017**, *96*, 044612. [[CrossRef](#)]
46. Oliveira, J.R.B.; Cappuzzello, F.; Chamon, L.C.; Pereira, D.; Agodi, C.; Bondi, M.; Carbone, D.; Cavallaro, M.; Cunsolo, A.; De Napoli, M.; et al. Study of the rainbow-like pattern in the elastic scattering of  $^{16}\text{O}$  on  $^{27}\text{Al}$  at  $E_{\text{lab.}} = 100$  MeV. *J. Phys. G Nucl. Part. Phys.* **2013**, *40*, 105101. [[CrossRef](#)]
47. Soukeras, V.; Pakou, A.; Cappuzzello, F.; Acosta, L.; Agodi, C.; Alamanos, N.; Bondi, M.; Carbone, D.; Cavallaro, M.; Cunsolo, A.; et al. Reexamination of  $^6\text{Li}+p$  elastic scattering in inverse kinematics. *Phys. Rev. C* **2015**, *91*, 057601. [[CrossRef](#)]
48. Ermamatov, M.J.; Ermamatov, M.J.; Linares, R.; Lubian, J.; Ferreira, J.L.; Cappuzzello, F.; Carbone, D.; Cavallaro, M.; Cubero, M.; de Faria, P.N.; et al. Comprehensive analysis of high-lying states in  $^{18}\text{O}$  populated with  $(t, p)$  and  $(^{18}\text{O}, ^{16}\text{O})$  reactions. *Phys. Rev. C* **2017**, *96*, 044603.
49. Pereira, D.; Linares, R.; Oliveira, J.R.B.; Lubian, J.; Chamon, L.C.; Gomes, P.R.S.; Cunsolo, A.; Cappuzzello, F.; Cavallaro, M.; Carbone, D.; et al. Nuclear rainbow in the  $^{16}\text{O}+^{27}\text{Al}$  system: The role of couplings at energies far above the barrier. *Phys. Lett. B* **2012**, *710*, 426. [[CrossRef](#)]
50. Cappuzzello, F.; Rea, C.; Bonaccorso, A.; Bondi, M.; Carbone, D.; Cavallaro, M.; Cunsolo, A.; Foti, A.; Orrigo, S.E.A.; Rodrigues, M.R.D.; et al. New structures in the continuum of  $^{15}\text{C}$  populated by two-neutron transfer. *Phys. Lett. B* **2012**, *711*, 347. [[CrossRef](#)]
51. Tudisco, S.; La Via, F.; Agodi, C.; Altana, C.; Borghi, G.; Boscardin, M.; Bussolino, G.; Calcagno, L.; Camarda, M.; Cappuzzello, F.; et al. Sicilia—Silicon carbide detectors for intense luminosity investigations and applications. *Sensors* **2018**, *18*, 7. [[CrossRef](#)]
52. Oliveira, J.R.B.; Moralles, M.; Flechas, D.; Carbone, D.; Cavallaro, M.; Torresi, D.; Acosta, L.; Agodi, C.; Amador-Valenzuela, P.; Bonanno, D.; et al. for NUMEN collaboration “First comparison of GEANT4 hadrontherapy physics model with experimental data for a NUMEN project reaction case. *Eur. Phys. J. A* **2020**, *56*, 153. [[CrossRef](#)]
53. Iazzi, F.; Ferrero, S.; Introzzi, R.; Pinna, F.; Scaltro, L.; Calvo, D.; Fisichella, M.; Agodi, C.; Cappuzzello, F.; Carbone, D.; et al. A new cooling technique for targets operating under very intense beams. *Trans. Eng. Sci.* **2017**, *116*, 61–70.
54. Capirossi, V.; Delaunay, F.; Fisichella, M.; Iazzi, F.; Introzzi, R.; Pinna, F. Study, fabrication and test of a special cooling system for targets submitted to intense ion beams. *Nucl. Instrum. Meth. A* **2018**, *954*, 161122. [[CrossRef](#)]
55. Pinna, F.; Calvo, D.; Capirossi, V.; Delaunay, F.; Fisichella, M.; Iazzi, F.; Introzzi, R. Design and test of an innovative static thin target for intense ion beams. *IL Nuovo Cim. C* **2019**, *42*, 67.
56. Sartirana, D.; Calvo, D.; Capirossi, V.; Ferrarese, C.; Iazzi, F.; Pinna, F.; For NUMEN Collaboration. Target Manipulation in Nuclear Physics Experiment with Ion Beams. In *Advances in Service and Industrial Robotics; Mechanisms and Machine Science*; Zeghloul, S., Laribi, M., Sandoval Arevalo, J., Eds.; Springer: Cham, Switzerland, 2020; Volume 84, p. 535.
57. Finocchiaro, P.; Acosta, L.; Agodi, C.; Altana, C.; Amador-Valenzuela, P.; Boztosun, I.; Brasolin, S.; Brischetto, G.; Brunasso, O.; Calabrese, S.; et al. For the NUMEN Collaboration. The NUMEN Heavy Ion Multidetector for a Complementary Approach to the Neutrinoless Double Beta Decay. *Universe* **2020**, *6*, 129. [[CrossRef](#)]
58. Calabretta, L.; Calanna, A.; Cuttone, G.; Agostino, G.D.; Rifuggiato, D.; Russo, A.D. Overview of the future upgrade of the INFN superconducting cyclotron. *Modern Phys. Lett. A* **2017**, *32*, 1740009. [[CrossRef](#)]
59. Calabretta, L.; Calanna, A.; Cuttone, G.; D’Agostino, G.; Rifuggiato, D.; Russo, A.D. Proceedings of the International Conference on Cyclotron and the R Applications. 2016. Available online: [www.accelconf.web.cern.ch/AccelConf/Cyclotrons2016/papers/moa02.pdf](http://www.accelconf.web.cern.ch/AccelConf/Cyclotrons2016/papers/moa02.pdf) (accessed on 16 March 2021).
60. D’Agostino, G.; Calabretta, L.; Calanna, A.; Rifuggiato, D. Proceedings of the International Conference on Cyclotron and Their Applications. 2016. Available online: [www.accelconf.web.cern.ch/AccelConf/Cyclotrons2016/papers/tuc03.pdf](http://www.accelconf.web.cern.ch/AccelConf/Cyclotrons2016/papers/tuc03.pdf) (accessed on 16 March 2021).
61. Calanna, A. High-intensity extraction from the Superconducting Cyclotron at LNS-INFN. *Il Nuovo Cimento* **2017**, *C40*, 101.
62. Shima, K.; Kuno, N.; Yamanouchi, M.; Tawara, H. Equilibrium charge fractions of ions of  $Z=4-92$  emerging from a carbon foil. *At. Data Nucl. Data Tables* **1992**, *51*, 173. [[CrossRef](#)]

63. Gallo, G.; Costa, G.; Allegra, L.; Messina, G.; Zappala, E. Proceedings of the International Conference on Cyclotron and Their Applications. 2016. Available online: [www.accelconf.web.cern.ch/AccelConf/Cyclotrons2016/papers/thp09.pdf](http://www.accelconf.web.cern.ch/AccelConf/Cyclotrons2016/papers/thp09.pdf) (accessed on 16 March 2021).
64. Tomic, S.S.; Samsonov, E.V. Analytical description of stripping foil extraction from isochronous cyclotrons. *Phys. Rev.* **2002**, *E65*, 036504.
65. Calabretta, L.; Calanna, A.; D'Agostino, G.; Rifuggiato, D.; Russo, A.D. IPAC 2017. Available online: [www.accelconf.web.cern.ch/AccelConf/IPAC2017/papers/wepva053.pdf](http://www.accelconf.web.cern.ch/AccelConf/IPAC2017/papers/wepva053.pdf) (accessed on 16 March 2021).
66. Russo, A.D.; Calabretta, L.; Cardella, G.; Russotto, P. Preliminary design of the new FRAGment In-flight SEparator (FRAISE). *Nucl. Instrum. Methods Phys. Res. Sect. B Beam Interact. Mater. At.* **2020**, *463*, 418–420. [[CrossRef](#)]
67. D'Agostino, G.; Calabretta, L.; Kleeven, W.; Rifuggiato, D. Proceedings of the International Conference on Cyclotron and Their Applications. 2019. Available online: [www.accelconf.web.cern.ch/AccelConf/ipac2019TUPTS023197](http://www.accelconf.web.cern.ch/AccelConf/ipac2019TUPTS023197) (accessed on 16 March 2021).
68. Neri, L.; Calabretta, L.; Rifuggiato, D.; D'Agostino, G.; Russo, A.D.; Gallo, G.; Allegra, L.; Costa, G.; Torrissi, G. 3D Magnetic Optimization of the New Extraction Channel for the LNS Superconducting Cyclotron. In Proceedings of the 22nd International Conference on Cyclotrons and their Applications (CYC2019), Cape Town, South Africa, 22–27 September 2019.
69. Radovinsky, A.; Calabretta, L.; Minervini, J.; Zhukovsky, A.; Michael, P.; Calanna, A. Design of a Superconducting Magnet for the LNS Cyclotron. *IEEE Trans. Appl. Supercond.* **2016**, *26*. [[CrossRef](#)]
70. Calanna, A.; Calabretta, L.; Rifuggiato, D.; D'Agostino, G.; Gallo, G.; Costa, G.; Allegra, L.; Russo, A.D. Study of the new return yoke for the upgraded Superconducting Cyclotron of INFN-LN IPAC 2017 Conference Proceeding with Peer Review. 2017. Available online: <http://iopscience.iop.org/issue/1742-6596/874/> (accessed on 16 March 2021).
71. Santopinto, E.; Garcia-Tecocoatzi, H.; Vsevolodovna, R.I.M.; Ferretti, J. Heavy-ion double-charge-exchange and its relation to neutrinoless double- $\beta$  decay. *Phys. Rev. C* **2018**, *98*, 061601. [[CrossRef](#)]
72. Cappuzzello, F.; Lenske, H.; Cunsolo, A.; Beaumel, D.; Fortier, S.; Foti, A.; Lazzaro, A.; Nociforo, C.; Orrigo, S.E.A.; Winfield, J.S. Analysis of the  $^{11}\text{B}$  ( $^7\text{Li}$ ,  $^7\text{Be}$ )  $^{11}\text{Be}$  reaction at 57 MeV in a microscopic approach. *Nucl. Phys. A* **2004**, *739*, 30. [[CrossRef](#)]
73. Lenske, H.; Bellone, J.I.; Colonna, M.; Lay, J.-A. Theory of single-charge exchange heavy-ion reactions. *Phys. Rev. C* **2018**, *98*, 044620. [[CrossRef](#)]
74. Bellone, J.I.; Burrello, S.; Colonna, M.; Lay, J.-A.; Lenske, H. Two-step description of heavy ion double charge exchange reactions. *Phys. Lett. B* **2020**, *807*, 135528. [[CrossRef](#)]